Controlling load-dependent contractility of the heart at the single molecule level

Chao Liu[1], Masataka Kawana[2], Dan Song[1], Kathleen M. Ruppel[1,3], and James A. Spudich[1*]

[1]Department of Biochemistry, Stanford University School of Medicine, Stanford, CA 94305, USA

[2]Department of Medicine, Division of Cardiovascular Medicine, Stanford University School of Medicine, Stanford, CA 94305, USA.

[3]Department of Pediatrics (Cardiology), Stanford University School of Medicine, Stanford, CA 94305, USA

*Correspondence to: jspudich@stanford.edu

Abstract

Concepts in molecular tension sensing in biology are growing and have their origins in studies of muscle contraction. In the heart muscle, a key parameter of contractility is the detachment rate from actin of myosin, which determines the time that myosin is bound to actin in a force-producing state and, importantly, depends on the load (force) against which myosin works. Here, we measure the detachment rate of single molecules of human β-cardiac myosin and its load dependence. We find that both can be modulated by both small molecule compounds and cardiomyopathy-causing mutations. Furthermore, effects of mutations can be reversed by introducing appropriate compounds. Our results suggest that activating vs. inhibitory perturbations of cardiac myosin are discriminated by the aggregate result on duty ratio, average force, and ultimately average power output and that cardiac contractility can be controlled by tuning the load-dependent kinetics of single myosin molecules.

Introduction

The ability to sense and respond to force is a fundamental feature observed across all scales of biology, from tissues[1,2], to cells[3,4], and to individual molecules[5-8]. Muscle contraction is a classic example in which tension sensing of the tissue [9] has its roots in the individual molecular motors working in every muscle cell – the myosin molecule.

Detachment rate is a key kinetic parameter describing myosin's actin-activated ATPase cycle because it determines the time myosin is bound to actin in a force-producing state. This rate depends on the force (load) against which myosin works as demonstrated in single molecule optical trap experiments with cardiac [10,11], skeletal [12], smooth [13], and non-muscle myosins [14-16]. The load-dependent detachment rate ($k_{det}(F)$) is a fundamental characteristic of every individual myosin molecule. As such, it determines whether a non-muscle myosin is a force sensor (myosin Ib) or a transporter (myosins V, Ic), while for muscle myosins, it defines the identity of the particular muscle (skeletal, cardiac, smooth). Even within a particular muscle type, different isoforms have different load-dependent kinetics adapted to their specific function. For instance, the beta isoform of cardiac muscle myosin is slower but has higher load-bearing ability than the alpha isoform [17], consistent with its dominant presence in the ventricles rather than the atria of the heart [18]. The cardiac myosin identity is so specifically tuned such that the relative composition of the alpha and beta isoforms changes in the failing heart [18]. Furthermore, replacement of one by the other had a detrimental effect in transgenic mice subjected to cardiovascular stress [19].

Thus, it is apparent that significant differences in the amino acid sequences of different myosin types dramatically change $k_{det}(F)$ to accommodate their molecular functions. However, it is not known whether small perturbations such as disease-causing mutations and small molecule drugs can control and alter the $k_{det}(F)$ in any specific myosin. Here, we address this question by measuring the effects of various small perturbations on the load-dependent kinetics of human β-cardiac myosin. Measurement of $k_{det}(F)$ of single striated muscle myosin molecules under physiological (~2 mM) ATP conditions had been challenging due to their short binding lifetime until the development of Harmonic Force Spectroscopy (HFS), which presented a simple and efficient solution without the need for fast feedback [11]. In the present study, we first demonstrate the robustness of the HFS method by measuring $k_{det}(F)$ for a population (n=36) of single molecules of human β-cardiac sS1, the motor domain (residues 1-808) of the myosin responsible for force production in the ventricles of the heart (hereafter referred to as myosin). We then tested the extent to which small molecule compounds affect $k_{det}(F)$. These compounds include both allosteric activators and an inhibitor of cardiac myosin, including the potential heart failure drug omecamtiv mecarbil (OM) [20], and the potential active-site therapeutic 2-deoxy-ATP (dATP) [21,22]. Next, we introduced mutations into β-cardiac sS1 that cause hypertrophic (HCM: D239N and H251N) or dilated (DCM: A223T, R237W and S532P) cardiomyopathies and measured their effects on $k_{det}(F)$. We further show that the effects of mutations can be reversed by adding the appropriate small molecule compounds. Finally, we discuss implications for cardiac myosin power production under these various perturbations.

Results

Harmonic Force Spectroscopy enables simple and efficient measurement of load-dependent kinetics on single molecules of human β-cardiac myosin

In Harmonic Force Spectroscopy (HFS) optical trap experiments, the lifetimes of binding events between a single myosin motor and actin under various loads can be directly measured in saturating (2 mM) ATP conditions [11]. The sample stage oscillates so that when myosin binds to actin, it immediately experiences a sinusoidally varying load with a certain mean value (Fig. 1A). Oscillation serves two essential purposes: 1) A range of mean loads, both positive and negative, is automatically applied over the course of many events by virtue of the randomness of where myosin initially attaches to actin (Fig. 1A). 2) Oscillation allows for the detection of short binding events of cardiac myosin to actin, which were previously more difficult to detect than longer events. In the unattached state, the dumbbell oscillates $\pi/2$ ahead of the stage due to fluid motion, and in the attached state the dumbbell oscillates in phase and with a larger amplitude due to stronger association with the oscillating stage (Fig. 1B). Therefore, events are detected automatically based on a simultaneous increase in oscillation amplitude above a threshold and a decrease in phase below a threshold (Fig. 1B). Unlike other methods which require feedback to apply a load [10,12,13,23], HFS enables detection of short events (>5 ms, one period of stage oscillation) and applies an immediate load to myosin regardless of the length of an event.

In the analysis of time trace data for a single myosin molecule, binding events are first detected, each defined by the duration t_s and mean force F (Fig. 1C). Events are then binned in force increments of ~1 pN so that the detachment rate for each bin $k_{det}(F)$ can be calculated by a maximum likelihood estimation (Fig. 1C inset). Since the load experienced by myosin during an event is sinusoidal with amplitude ΔF and mean F, the dependence of the detachment rate k_{det} on force is given by the force-dependent Arrhenius equation with a harmonic force correction:

$$k_{\mathrm{det}}(F,\Delta F) = k_0 I_0\left(\frac{\Delta F \delta}{k_B T}\right)\exp\left(-\frac{F\delta}{k_B T}\right) \qquad \text{Eqn. 1}$$

where k_0 is the rate at zero load, δ is the distance to the transition state of the rate limiting step in the bound state (a measure of sensitivity to force), k_B is the Boltzmann constant, T is temperature, and I_0 is the zeroth-order modified Bessel function of the first kind (to correct for the harmonic force). This equation is fitted to the detachment rates $k_{det}(F)$ with the parameters k_0 and δ to obtain the loaded curve for a single myosin molecule (Fig. 1D).

Measurements of a population (n=36) of single molecules of human β-cardiac myosin yielded the mean values $k_0 = 102 \pm 4\ s^{-1}$ and $\delta = 1.31 \pm 0.03$ nm (standard error of mean, s.e.m.) (Fig. 1E, F), consistent with previously reported values [10,11]. The HFS method allowed us to produce a load-dependent curve for each molecule rather than one from events aggregated across multiple molecules, therefore producing the distribution of the population and revealing inherent molecule-to-molecule differences (Fig. 1E, F).

Allosteric effectors of human β-cardiac myosin slow down ensemble actin-sliding velocity

We investigated four allosteric activators (A2876, C2981, D3390, OM), one allosteric inhibitor (F3345), and the active-site substrate dATP as small molecule effectors of cardiac myosin (Fig. 2A). dATP, a potential heart failure therapeutic [21], acts in place of ATP and has been shown to enhance cardiac myosin's ATPase activity [22]. A2876, C2981, and D3390 were derived from hits discovered from an ATPase screen using bovine cardiac subfragment-1 (S1) and regulated thin filaments (purified bovine actin, tropomyosin, and troponins C, I, and T), and F3345 was derived from a hit discovered from an ATPase screen using bovine myofibrils, all by MyoKardia, Inc. OM, an investigational drug in phase III clinical trials for heart failure [20,24] (GALACTIC-HF, www.clinicaltrials.gov NCT02929329), has been proposed to increase ensemble force by increasing myosin's duty ratio, the fraction of time spent in the strongly-bound, force producing state [17,25-27]. The rate of ADP release normally determines the strongly-bound state time, but surprisingly, OM was found to delay the power stroke [27] without affecting this rate [20,25-27]. To clarify OM's mechanism of action, we used HFS to directly measure whether the drug causes a single cardiac myosin molecule to stay bound longer to actin.

To determine the effects of the compounds when a single myosin molecule has a compound bound, a saturating concentration of compound was required. To determine this concentration, we measured the dose-dependent effects of the compounds on the actin-sliding velocities of human β-cardiac myosin in an in vitro motility assay [17,28]. Surprisingly, both activators and inhibitors slowed down velocities, but to different extents (Fig. 2B). In particular, OM had the most dramatic effect with a median effective concentration (EC_{50}) ~0.1 μM, in close agreement with previous measurements [17,25,26]. Activator A2876 had no effect on the velocity beyond that from DMSO alone (see methods).

Guided by the motility measurements, we performed all subsequent single-molecule experiments that involve allosteric effectors at a concentration of 25 μM in 2% DMSO.

Small molecule compounds modulate the load-dependent kinetics of single molecules of human β-cardiac myosin

We measured the effects of the small molecule compounds on the load-dependent detachment rates of single molecules of human β-cardiac myosin using HFS (Fig. 3). For clarity, we present only the average load-dependent kinetics curve for each condition in Fig. 3B (for curves of the individual molecules, see Fig. S2). Values of k_0 and δ are summarized in Tables 1 and S1. When dATP was used as myosin's substrate, the rate k_0 increased (dATP: k_0 = 168 ± 7 s^{-1} vs ATP: 102 ± 4 s^{-1}) while δ, a measure of the sensitivity to force, did not change significantly (dATP: δ = 1.5 ± 0.1 nm vs ATP: δ = 1.31± 0.03 nm, p = 0.13), in close agreement with experiments performed using bovine cardiac heavy meromyosin (HMM) (Tomasic I., Liu C., Rodriguez H., Spudich J.A., Bartholomew Ingle S.R., manuscript in preparation). Compound A2876 had no effect beyond that from DMSO. This result is consistent with observations that A2876 has no effect on the actin-activated ATPase of purified bovine cardiac myosin and actin, but only activates myosin's ATPase activity in the presence of regulated thin filaments, suggesting possible interactions with the tropomyosin-troponin complex (R. Anderson, MyoKardia unpublished results). The activators C2981, D3390, and OM decreased k_0 dramatically (C2981: k_0 = 23 ± 1 s^{-1}, D3390: k_0 = 55 ± 3 s^{-1}, OM: k_0 = 12 ± 1 s^{-1}) while also decreasing δ (C2981: δ = 0.79 ± 0.05

nm, D3390: δ = 0.93 ± 0.03 nm, OM: δ =0.26 ± 0.05 nm) (Fig. 3A), resulting in a much lower and flatter curve that is less sensitive to force (Fig. 3B). All three of these activators probably interact directly with myosin, and lowering of both k_0 and δ may be a general characteristic of myosin-associated activators. In contrast, the inhibitor F3345 decreased the detachment rate (k_0 = 36 ± 2 s^{-1}) without changing the force sensitivity (δ = 1.27 ± 0.06 nm), suggesting a possible mechanism of action distinct from the activators. Taken together, we found that small molecule effectors can modulate the detachment rate and load sensitivity of cardiac myosin to various degrees.

Cardiomyopathy-causing mutations alter the load-dependent kinetics of single molecules of human β-cardiac myosin

We next measured the effects of various cardiomyopathy-causing mutations on the load-dependent detachment rates of single molecules of human β-cardiac myosin using HFS (Fig. 4 and S3, Tables 1 and S1). Two early-onset HCM mutations (D239N and H251N) were found previously to cause myosin to have higher actin sliding velocities in the in vitro motility assay [29]. Consistent with their hyperactivities, these two HCM mutants exhibited faster detachment rates than the wild-type (WT) protein at the single-molecule level (D239N: k_0 = 140 ± 3 s^{-1}, p = 0.04; H251N: 152 ± 7 s^{-1}, p = 0.02) and slight effects on force sensitivity (D239N: δ = 1.40 ± 0.03 nm, p = 0.04; H251N: δ = 1.53 ± 0.08 nm, p = 0.02). Of the three DCM mutations we studied, A223T did not change the load-dependent detachment rate compared to WT myosin (k_0 = 104 ± 4 s^{-1}, p = 0.17; δ = 1.48 ± 0.09 nm, p = 0.13), R237W increased the rate without changing force sensitivity (k_0 = 155 ± 15 s^{-1}, p = 0.004; δ = 1.25 ± 0.06 nm, p = 0.43), and S532P decreased the rate slightly without changing force sensitivity (k_0 = 80 ± 8 s^{-1}, p = 0.02; δ = 1.37 ± 0.06 nm, p = 0.57). Thus, point mutations that cause disease can indeed alter the load-dependent kinetics of cardiac myosin to various degrees, but whether the mutation is clinically HCM or DCM does not dictate the direction of the change (Fig. S6). Interestingly, the DCM mutants R237W and S532P both had greater molecule-to-molecule variabilities in k_0 compared to WT and other mutants (Fig. 4A and S3), suggesting that these mutations may cause a disruption in protein folding that affects individual myosin molecules in a population to different extents.

The effects of cardiomyopathy-causing mutations can be reversed by appropriate small molecule compounds

If an effect of a disease-causing mutation is to alter the detachment rate, then we hypothesized that a small molecule compound with the opposite effect on WT myosin will reverse the alteration caused by the mutation, provided the mutation does not interfere with the action of the compound. To test our hypothesis, we first measured the effects of the inhibitor F3345 on the load-dependent kinetics of each of the two HCM mutants. As expected, we observed a dramatic decrease in the detachment rates of both HCM mutants (D239N + F3345: k_0 = 24 ± 2 s^{-1}, H251N + F3345: 20 ± 2 s^{-1}) without a significant change in force sensitivity (D239N + F3345: δ = 1.35 ± 0.08 nm, H251N + F3345: 1.27 ± 0.05 nm) (Fig. 4 and S3, Table S1). Next, since the DCM mutant R237W has a faster detachment rate than WT, we applied the activator OM and found a similarly dramatic reversal (k_0 = 8 ± 1 s^{-1}), this time with a much lower force sensitivity (δ = 0.21 ± 0.06 nm) as expected from the effects of OM (Fig. 4 and S3, Table S1). Finally, since S532P had a lower detachment rate than WT, we found that replacement of ATP with dATP reversed the mutation's effect (k_0 = 170 ± 6 s^{-1}). Since saturating compound concentrations (25

μM allosteric effectors or 2 mM dATP) reversed the effects of mutations beyond WT levels (Fig. 4), we expect by kinetic reasoning that appropriate lower concentrations can adjust the detachment kinetics of mutants to match that of WT myosin if desired.

Taken together, we have found that both small molecule effectors and disease-causing mutations in human β-cardiac myosin can independently and in combination modulate the behavior of single myosin molecules under load. This allows one to have a fine-tuned control over the fundamental load-dependent kinetics curve that defines cardiac myosin.

Single molecule load-dependent kinetics is the basis of the ensemble force-velocity relationship in β-cardiac myosin

In ensemble motility, the sliding velocity of an actin filament is limited by how fast the attached myosin molecule can let go of it, i.e., the detachment rate of myosin. Therefore, ensemble velocities measured by the in vitro motility assay should be proportional to the single molecule detachment rates measured by the optical trap. As expected, ensemble velocities were found to be linearly related to the detachment rate k_0 with a slope of 8.9 nm and $R^2 = 0.81$ (Fig. 5A). In simplest terms, since unloaded velocity $v = d/t_s = d*k_0$, where d = step size and t_s = strongly bound state time, the slope obtained from this linear fit can be interpreted as the effective step size of myosin in the ensemble. This effective step size (8.9 nm) is greater than the value from direct step size measurements on single cardiac myosin molecules (~7 nm) [10,30,31] because the non-zero load-dependence (δ) of cardiac myosin results in faster detachment rates in the ensemble [32]. Interestingly, the activators and HCM mutants lie on or above the fitted line while the inhibitor F3345 and DCM mutants lie below it (Fig. 5A). This presents a possible distinction between the two groups in which activating perturbations produce greater coordinated movement in the ensemble than predicted by single molecule detachment rates while inhibitory perturbations result in less enhancement.

In addition to k_0, our data revealed differences in force sensitivity (δ) under different perturbations to cardiac myosin at the single molecule level (Fig. 3A, 4A). Therefore, we asked whether changes to force sensitivity of single molecules result in similar findings on the ensemble level. We measured ensemble force sensitivity by a loaded in vitro motility assay [17]. In this assay, utrophin on the surface binds to actin to provide the load against which myosin must overcome in moving actin filaments. Increasing concentrations of utrophin increase load and thus decreases actin sliding velocity. This gives an ensemble force-velocity curve (Fig. S4). The concentration of utrophin K_s required to reduce velocity by half is therefore a measure of force sensitivity. As expected, we found that K_s is inversely proportional to δ (Pearson correlation coefficient = -0.94) (Fig. 5B and S4). As single myosin molecules become insensitive to load (smaller δ), such as the cases of the activators OM, C2981, and D3390, higher concentrations of utrophin are required to reduce the ensemble velocities by a half.

In conclusion, we have found that the load-dependent kinetics inherent to each single molecule of cardiac myosin can be modulated by various small molecule compounds and mutations. This single molecule characteristic underlies the force-velocity relationship exhibited in ensemble.

Discussion

Large sequence differences between various types of myosin lead to dramatically different scales of the load-dependent detachment rate. Myosin I [15,16], V [14], smooth [13], and β-cardiac [10,11] isoforms have distinct rates and force sensitivities ranging from k_0 ~ 1 to 100 s^{-1}, and δ ~ 1 to 12 nm. Here, we explored whether changes to the load-dependent rate can be made via small perturbations in the form of small molecule compounds and cardiomyopathy-causing single missense mutations in human β-cardiac myosin. The results lie across the spectrum: not all perturbations changed the single molecule load-dependent detachment rates (activator A2876, DCM mutant A223T), while the rest modulated the curve to various extents (Fig. 3, 4, and S6). Modulation was seen in the rate at zero load k_0 (~ 10 to 170 s^{-1}) and/or the force sensitivity δ (~ 0.2 to 1.5 nm). Furthermore, the effects of mutations could be reversed by an appropriate compound (Fig. 4). Thus we have observed fine tuning of the load-dependent kinetics on single molecules of cardiac myosin. In oversimplified terms, we can control cardiac contractility at the single molecule level.

Perturbations to myosin change its load-dependent detachment rates through different steps in the ATPase cycle

Any step in the strongly-bound state may be affected by the compounds and mutations. ADP release is the rate-limiting step of the strongly-bound state under unperturbed circumstances for WT cardiac myosin. This is likely the acted-upon step for dATP, inhibitor F3345, and mutations since the transition state distance (δ) for those conditions remained close to that of WT myosin without treatment (Fig. 3A, 4A, and Table 1). Furthermore, it has been measured by stopped flow experiments of bovine cardiac HMM that the faster nucleotide release rate when dATP is used in place of ATP matches the detachment rate measured on single molecules (Tomasic I., Liu C., Rodriguez H., Spudich J.A., Bartholomew Ingle S.R., manuscript in preparation). For the activators C2981, D3390, and OM, the significantly smaller δ (Fig. 3A and Table 1) may suggest a new rate limiting step with a different transition state. Alternatively, the compounds may have simply changed the transition state of ADP release to yield smaller distance. Future kinetic studies are needed to distinguish between these models and illuminate the precise steps at which the compounds act.

For OM, it has been shown that the drug stabilizes the pre-powerstroke state in which myosin is ready to bind to actin [33], accelerates phosphate (P_i) release [20,25,27], then delays the power stroke while myosin is in the actin-bound state [27]. Structural data suggests OM unbinds before the stroke [33], thus leaving the ADP release rate unaffected [20,25-27]. In our study, we measured an overall large increase in the lifetime ($1/k_{det}$) of the bound state, consistent with the previously observed delay in powerstroke. However, calculation of the attachment rate k_{attach} defining the lifetime of the unbound state gives a value (2 s^{-1}, see Table 1 and discussion in the next section) much smaller than reported P_i release rates (~20-30 s^{-1}) [25,27]. This discrepancy suggests P_i release is not the rate-limiting step in the unbound state. Unlike solution measurements, measurement of event lifetimes on single myosin molecules provides direct determination of the attachment and detachment rates. But at the same time, a limitation of our measurement is an inability to determine the precise steps affected; our data does not show whether the power stroke and/or the ADP release rate are prolonged.

However, it can be argued that whether an effector changes the time spent in the bound state before the stroke or after the stroke, the same result is achieved: the overall bound time is prolonged, and it is this overall bound time that limits ensemble velocity and determines force production.

Single molecule vs. ensemble observations

Fitting with the above statement that the overall bound time determines ensemble velocity, we found a strong linear relationship between single molecule detachment rate and ensemble velocity (Fig. 5A). Activators C2981 and D3390 and inhibitor F3345 may act in steps of the ATPase cycle different from those of OM, but the result is the same - a prolonged strongly bound state time. This manifests itself similarly: a slowing of ensemble velocity, despite differences in the details of the mechanism. In this way, the single molecule detachment rate k_0 does truly dictate to a large extent motility velocity for cardiac myosin.

Since small molecule effectors may prolong the strongly bound state by slowing the kinetics of different steps, it is not surprising that the distances to the transition state are also altered. While the mechanistic details may vary with different compounds or mutations, the net result is a change in δ, the parameter that encapsulates force sensitivity. When the force sensitivity inherent to a single molecule is changed, the result is reflected at the ensemble level (Fig. 5B). Thus we find that different mechanisms of changing k_0 and δ can lead to the same ensemble force-velocity behavior (Fig. 5).

While the ensemble observation correlates well with predictions from single molecule data, not all the variation observed in the ensemble case can be explained by the current single molecule model (Fig. 5). For example, why do HCM mutations and activators move faster in motility than predicted by detachment rates alone, while DCM mutations and the inhibitor F3345 have the opposite effect? A more sophisticated model of ensemble motility from single molecule parameters will be explored in future work.

One parameter for which we have not yet measured effects of perturbations is myosin's step size *d*. Previous studies show little or no significant change to *d* by HCM or DCM mutations [30,31,34] (Choe E., Spudich J.A., and Ruppel K.M., unpublished results), but that may not be the case for all perturbations studied in this paper. Ongoing and future studies will answer this question. In addition, one may ask whether myosin is truly making a stroke under an applied load. Although we cannot observe the working stroke using HFS, we do believe that myosin is able to stroke because we apply forces below ~5-6 pN (Fig. 1C). It has been shown for skeletal muscle myosin that the stroke size remains the same at ~5 nm up to the isometric force of 5.7 pN [12]. This was found to be true when very short events (<1 ms) corresponding to short, unproductive binding were excluded from the analysis. In HFS, the stage oscillation of 200 Hz set our lower detection limit at 5 ms (one period), so all events included in our analysis have lifetimes greater or equal to 5 ms and therefore are expected to have productive working strokes. However, direct observation of a stroke under load would require an ultrafast feedback optical trap system [12].

We have found that small perturbations, activating or inhibitory, can increase, decrease, or not affect the detachment rates (Fig. 3, 4, and S6). While this may be expected given that compounds and mutations can act via different mechanisms of action, the question remains: what

distinguishes one group from the other? A heart containing an HCM mutation (eg. H251N) undoubtedly is hyper-contractile [35] compared to one bearing a DCM mutation (eg. R237W) despite both having faster detachment rates. Armed with knowledge of their load-dependent kinetics, we believe that the answer lies in an assessment of the resulting duty ratio, average force, and power output, as explained in the following section.

Implications of single-molecule load-dependent kinetics on power production by β-cardiac myosin

The duty ratio is the time myosin spends in the strongly bound state t_s divided by its entire cycle t_c and is an important parameter because it represents the fraction of time myosin is in a force producing state. The entire cycle is made up of time in the strong and weak states, t_s and t_w, respectively. The duty ratio as a function of load force F can be expressed as

$$r(F) = \frac{t_s}{t_c} = \frac{t_s}{t_s + t_w} = \frac{1/k_{\mathrm{det}}(F)}{1/k_{\mathrm{det}}(F) + 1/k_{attach}} = \frac{k_{attach}}{k_{attach} + k_{\mathrm{det}}(F)} \qquad \text{Eqn. 2}$$

where k_{attach} describes the lifetime of the weak binding state and is assumed to be independent of force since myosin cannot yet sense any load on actin when unbound. k_{attach} can be calculated by

$$k_{attach} = \left(\frac{1}{k_{cat}} - \frac{1}{k_{\mathrm{det}}(F=0)} \right)^{-1} = \left(\frac{1}{k_{cat}} - \frac{1}{k_0} \right)^{-1} \qquad \text{Eqn. 3}$$

where k_{cat} is measured by steady state ATPase. We know the values of all variables in these equations: $k_{det}(F)$ given by Eqn. 1 is measured by HFS in this study, k_{cat} is measured in an actin activated ATPase assay in this study (Table 1 and Fig. S5) and others [17,29] (Choe E., Spudich J.A., and Ruppel K.M., unpublished results). Therefore we can calculate the duty ratio as a function of load force (Fig. 6A). Values of k_0, δ, k_{cat}, and k_{attach} used are given in Table 1. Interestingly, we find that the duty ratios of the activators and HCM mutations in general lie above those of the inhibitor and DCM mutations. This result is consistent with physiological expectations that HCM mutations and activators cause myosin to have a higher duty ratio, while DCM mutations and inhibitors result in the opposite [25-27,33,36]. The inhibitor F3345 is an outlier whose curve lies among those of the activators/HCM's. Compared to the absence of small molecule compounds, OM dramatically increases the duty ratio of cardiac myosin even at low forces, consistent with previous studies which proposed that it causes myosin to spend a much

greater fraction of time in the strongly bound state [25-27,33]. At higher forces, its duty ratio does not increase as much as that of others due to its low force sensitivity (δ) (Fig. 3). Surprisingly, two of the activators (C2981 and D3390) increased the duty ratio even more dramatically than OM at both high and low forces. Furthermore, because their force sensitivities were not as low as that of OM (Fig. 3), their duty ratios increased more steeply with increasing force (Fig. 6A).

Average force is the load force F against which a single molecule was able to stroke multiplied by the duty ratio:

$$F_{av}(F) = Fr(F) \qquad \text{Eqn. 4}$$

The average force myosin produces increases with load force until the isometric force, taken to be 6 pN here [12] (Fig. 6B). As expected, the activators C2981, D3390 and OM increased the average force the most because they had the largest increase in duty ratio. Similar to duty ratio, calculation of the average force broadly discriminates the activators and HCM mutations from the inhibitor and DCM mutations.

Finally we calculate the average power produced by a single myosin:

$$\begin{aligned} P_{av}(F) &= F_{av}(F)dk_{\text{det}}(F) \\ &= Fdk_{\text{det}}(F)r(F) \end{aligned} \qquad \text{Eqn. 5}$$

where step size d is taken to be 7 nm. Here again, HCM and activators overall segregate from DCM mutations and inhibitors (Fig. 6C). The activator OM is the notable exception: it causes decreased power despite a higher average force because of its much slower kinetics. This can help explain the effects of OM observed at the organ level: the predicted higher average force is consistent with an increase in peak time-dependent elastance of the left ventricle (a measure of LV contractility) and stroke volume, while the slower kinetics is consistent with a longer time to maximum pressure and a longer time in systole [20,24].

Although our molecular findings in the case of OM are consistent with clinical observations, as discussed above, it is important to note that the high dose of OM we used in our experiments does not reflect the physiological dose used in animal or clinical studies. The saturating dose of OM was necessary for our single molecule experiments because we wanted to study myosin-actin events in which the compound is bound. At this high concentration, OM caused a decrease in the calculated power. A careful balance of OM's slow kinetics must be and is considered in clinical trials in order to achieve an increase in power. Finding the optimal degree of alteration in myosin function is critical in modulating ventricular function as a whole.

The k_{cat} term in the above equations should be measured in future studies on HMM rather than sS1 in order to encapsulate the term N_a, the number of available heads. Mutations on the myosin mesa [37] and compounds which regulate the interacting heads motif may change the proportions of the folded back state [38-40] thus changing k_{cat} measured for HMM while showing no change for sS1. In addition, other factors that build a more complex, comprehensive system (eg. regulated thin filament, myosin binding protein C) can also modulate the folded back state and thus change k_{cat}. These unaccounted-for complexities may explain why the compound A2876 showed no significant change from WT/DMSO in all experiments and the power calculation performed in

this study using the simple purified actin-activated myosin system (Fig. 2, 3, 6, and S5), yet was discovered as an activator from an ATPase screen using regulated thin filaments.

Given the above considerations, we propose a model in which activating vs inhibitory perturbations of cardiac myosin are discriminated by the aggregate result on duty ratio, average force, and ultimately average power (Fig. 7). While the load-dependent detachment rate is an essential parameter since it determines the time myosin spends in a strongly bound, force producing state, it alone cannot distinguish the two types of perturbations. The steady state k_{cat} cannot, by itself, distinguish them either. When both are taken into account by a calculation of the duty ratio, average force, or average power, then the distinction is made. To build a comprehensive understanding of the molecular mechanism underlying muscle contraction, these calculations takes into consideration all the parameters of force production: load force F, the load-dependent detachment rate $k_{det}(F)$, the overall cycle rate k_{cat}, the number of functionally available heads N_a (included in k_{cat}), and the step size d.

Recent studies on the HCM mutations R453C [30], R403Q [31], and three in the converter domain [41] found variable changes to parameters of force production (without $k_{det}(F)$ measurements) which do not clearly point to a hyper-contractile phenotype. Future studies measuring $k_{det}(F)$ for these mutants and others will illuminate whether molecular hyper-contractility and hypo-contractility are indeed the respective underlying effects of HCM and DCM.

Methods

Small molecule compounds were a generous gift from MyoKardia Inc. (South San Francisco). They are stored at 10 mM in 100% DMSO at 4 °C.

Protein preparation

Construction, expression and purification of the WT and mutated recombinant human β-cardiac myosin sS1s are described in detail elsewhere [29,30]. Briefly, a truncated version of *MYH7* (residues 1 – 808), corresponding to sS1, with either a C-terminal enhanced green fluorescent protein (eGFP) or a C-terminal eight-residue (RGSIDTWV) PDZ-binding peptide was co-expressed with myosin light chain 3 (*MYL3*) encoding human ventricular essential light chain (ELC) and containing an N-terminal FLAG tag (DYKDDDDK) and tobacco etch virus (TEV) protease site in mouse myoblast C2C12 cells using the AdEasy Vector System (Obiogene Inc.). The myosin heavy chain with its associated FLAG-tagged ELC was first purified from clarified lysate with anti-FLAG resin (Sigma). After cleaving off the FLAG tag with TEV protease, the human β-cardiac sS1 was further purified using anion exchange chromatography on a 1 mL HiTrap Q HP column (GE Healthcare). Peak fractions were eluted with column buffer (10 mM Imidazole, pH 7.5, ~200 mM NaCl, 4 mM $MgCl_2$, 1 mM DTT, 2 mM ATP and 10% sucrose) and concentrated by centrifugation in Amicon Ultra-0.5 10 kDa cutoff spin filters (EMD Millipore) before being stored at -80 °C. The purity of the protein was confirmed using SDS-PAGE (Fig. S1). Frozen proteins exhibited similar activities in the motility, single-molecule, and ATPase assays compared to their fresh counterparts, as seen in previous work [41].

Deadheading myosin

Myosin protein used for motility and trap experiments was further subjected to a "deadheading" procedure to remove inactive heads. Myosin was mixed with 10x excess of unlabeled F-actin on ice for 5 min, followed by addition of 2 mM ATP for 3 min, then centrifuged at 95K rpm in a TLA-100 rotor (Beckman Coulter) at 4 °C for 20 min. The supernatant was collected to be used in the motility and trap experiments. Myosin used in the ATPase assay was not subjected to deadheading.

Actin-activated ATPase

Purified bovine cardiac G-actin provided by MyoKardia Inc. was freshly cycled to F-actin by extensive (4 times over 4 days) dialysis in ATPase buffer (10 mM Imidazole, pH 7.5, 5 mM KCl, 3 mM $MgCl_2$ and 1 mM DTT) to remove any residual ATP up to a week before each experiment. The monomeric concentration of F-actin was determined by measuring the absorbance of a serial dilution of the actin in 6 M guanidine hydrochloride both at 290 nm with an extinction coefficient of 26,600 M^{-1} cm^{-1} and at 280 nm with an extinction coefficient of 45,840 M^{-1} cm^{-1} in a spectrophotometer (NanoDrop). Full-length human gelsolin was added to actin at a ratio of 1:1000 to reduce the viscosity of the actin and thereby decrease pipetting error at higher actin concentrations without affecting the ATPase activity [30]. The steady-state actin-activated ATPase activities of freshly prepared human β-cardiac sS1-eGFP were determined using a colorimetric readout of phosphate production [42]. In this assay, reactions containing sS1 at a final concentration of 0.01 mg mL^{-1}, 2 mM ATP or dATP, and actin at concentrations ranging from 2 to 100 μM were performed at 23°C with plate shaking using a microplate spectrophotometer (Thermo Scientific Multiskan GO). Prior to the start of each reaction, sS1s were incubated on ice with 25 μM of the indicated type of small molecule compound in 2% DMSO for 5 min. ATP or

dATP was added at t = 0, and four additional time points up to 30 min were measured subsequently for each actin concentration. The rate of sS1 activity was obtained by linear fitting the phosphate signal as a function of time and converted to activity units using a phosphate standard.

A set of experiments measuring all conditions (dATP and compounds) on WT sS1-eGFP were performed on the same day that myosin was purified to ensure that conditions can be directly compared to each other without variation due to different protein preparations. Each experiment of each condition was performed in duplicates or triplicates. The error on each data point (ATPase activity at a certain actin concentration) represents the s.e.m. of the replicates. The Michaelis-Menten equation was fitted to determine the maximal activity (k_{cat}) and the actin concentration at half-maximum (apparent K_m for actin). Data from one day is shown in Fig. S5A. The k_{cat} values from each day's experiment are averaged and presented in Table 1 along with their s.e.m.'s. Here we performed two sets of experiments using two protein preparations and a total of 5-7 replicates. Since each set of experiments measured all conditions on the same day using the same protein prep, we used the paired t-test to test for significance (Table 1). We also performed a Michaelis-Menten fit to the aggregated data from both days (Fig. S5B).

In vitro motility

The basic method followed our previously described motility assay with some modifications [28,31,41]. Two to three slides were used under 8 to 12 different concentrations of small molecules per set of experiment. Normalization of velocity was done using the velocity of WT control from the same set of experiments. For loaded in vitro motility assays, two to three slides were used under 8 to 12 different concentrations of utrophin to obtain a full curve with each run of an experiment. Movies were analyzed using FAST, and velocities reported are MVEL with 20% tolerance, as described previously [17]. Each experiment tracked ~400 to ~1900 actin filament movements, and the same condition was repeated. For unloaded velocity, mean +/- standard mean of error from the two experiments are plotted against compound concentration (Fig. 2). After myosin was attached to the motility surface and washed with BSA-containing assay buffer, Final GO solution that contained a designated concentration of small molecule and 0.5% DMSO was added. The myosin was incubated with the small molecule in Final GO for at least 5 minutes before movies were taken. The amount of time the Final GO was incubated in the chamber before movies were taken did not affect the velocity (data not shown). DMSO had minimal effect on velocity (2% DMSO had a 10% reduction in velocity). All experiments were performed at 23 °C.

Single molecule measurements of load-dependent detachment rates

Measurements were performed using the Harmonic force spectroscopy (HFS) method in a dual beam optical trap [11].

Sample chamber preparation. The sample chamber was built on a glass coverslip spin-coated first with 1.6 µm-diameter silica beads (Bang Laboratories) as platforms and then with a solution of 0.1% nitrocellulose 0.1% collodion in amyl acetate. The flow channel was constructed by two double-sided tapes between a glass slide and the coverslip. Experiments were performed at 23 °C. GFP antibody (Abcam ab1218) at a final concentration of 1 - 3 nM diluted in assay buffer (AB) (25 mM imidazole pH 7.5, 25 mM KCl, 4 mM $MgCl_2$, 1 mM EGTA, and 10 mM DTT)

was flowed into the channel to bind the surface for 5 min, followed by washing and blocking with 1 mg ml^{-1} BSA in AB (ABBSA) for 5 min. Dead-headed human β-cardiac myosin sS1-eGFP diluted to a final concentration of ~10-50 nM in ABBSA was flowed in next and allowed to saturate GFP antibody binding sites for 5 min. Then unbound myosin was washed out with ABBSA. Lastly, the final solution was flowed in consisting of 2 mM ATP, 1 nM TMR-phalloidin-labelled biotinylated actin (Cytoskeleton) filaments, an oxygen-scavenging system (0.4% glucose, 0.11 mg ml^{-1} glucose oxidase, and 0.018 mg ml^{-1} catalase), and 1 μm-diameter neutravidin-coated polystyrene beads (ThermoFisher) diluted in ABBSA. The chamber was sealed with vacuum grease. For experiments with 2-deoxy-ATP, 2 mM 2-deoxy-ATP was used in place of ATP. For experiments with other small molecule compounds, ABBSA contained 2% DMSO and 25 μM compound.

HFS experiment. Details of the technique have been presented elsewhere [11]. Two neutravidin beads were trapped in two trap beams. The beads were moved in ~57 nm steps in a 9x9 raster scan using acousto-optic deflectors while their displacements were recorded both in brightfield (in nm) and with quadrant photodiode (QPD) detectors (in voltage) to produce a voltage-to-nm calibration. The stiffness of each trap beam was calculated by the equipartition method and was typically ~0.09 pN nm^{-1} in these experiments. After this calibration, an actin filament was stretched to ~5-10 pN pre-tension between the two trapped beads to form a "dumbbell." We sinusoidally oscillated the piezoelectric stage with amplitude 50 nm at 200 Hz. The dumbbell was lowered near a platform bead to check for binding to a potential myosin on the platform, as indicated by large, brief increases in the position amplitudes of the trapped beads due to stronger association with the oscillating stage. We typically explored ~5-10 platform beads before robust interactions were observed, suggesting that the GFP antibody and myosin concentrations used in this study resulted in sufficiently low number of properly-oriented molecules on the surface such that events observed were likely due to a single myosin. The positions of the trapped beads and the piezoelectric stage were recorded at 50 kHz sampling frequency. We recorded data on each molecule for ~10 min and used each slide for 1.5-2 hr. We did not observe slowing down of motor during the 10-min recording for one molecule nor for multiple molecules on one slide during a 2 hr experiment, suggesting that the 2 mM ATP was not significantly depleted despite our foregoing an ATP regeneration system.

HFS data analysis. The theory of the HFS method and the data processing details have been presented elsewhere [11]. In summary, in the unattached state, the dumbbell oscillates π/2 ahead of the stage due to the fluid motion while in the attached state the dumbbell oscillates in phase and with a larger amplitude due to stronger association with the stage. Therefore, events are detected based on a simultaneous increase in oscillation amplitude above a threshold (~15 nm) and a decrease in phase below a threshold (~0.5 rad) for at least one full stage oscillation period. Several additional filtering of events are applied to minimize false positives. The final number of events for each molecule ranged from ~300-1000. For each event, the mean force due to each trap is calculated as the bead position averaged over the duration of binding multiplied by the trap stiffness. The total mean force on myosin is the sum of the two mean forces. A range of forces, both positive and negative, is automatically applied to myosin because binding can occur anywhere in the cycle of oscillation. For each molecule, events are binned by force in ~1 pN increments, and a maximum likelihood estimation (MLE) is performed for each bin to obtain the detachment rate for the mean force of the bin, $k_{det}(F)$. The error on $k_{det}(F)$ is calculated from the

variance of the MLE as the inverse Fisher information. This results in a plot of $k_{det}(F)$ vs. F to which we perform a weighted least-squares fit of Eqn. 1 using k_0 and δ as fitting parameters. Theoretical errors on the estimates for k_0 and δ are calculated from the inverse Fisher information matrix. Thus we have k_0 and δ and their errors for each molecule. Then, values of k_0 and δ from each molecule are averaged weighted by their errors (variance) to obtain mean values for each condition. The errors on these mean values are calculated as the s.e.m.

Normalization of in vitro motility results

The range of WT velocities from different protein preparations was 600-1100 nm/s, and this variability has also been observed previously [41]. Because of this, velocities and K_s of different conditions (compounds and mutations) were normalize-adjusted by each of their WT controls. For example, if condition x had a velocity of v_x, and its corresponding WT control had a velocity of $v_{x\_control}$, then the adjusted velocity was $v_{x\_adjusted} = v_x * v_{WT}/v_{x\_control}$ where v_{WT} is the velocity of the WT measured in this study against which everything else is compared.

Calculations of duty ratio, average force, and average power

Calculations are given by Eqn. 2-5 using values in Table 1. Values and errors referenced from other studies are normalized by each of their corresponding WT protein controls. Errors in k_{attach} are calculated as propagated errors derived from Eqn. 3.

References

1 Petridou, N. I., Spiro, Z. & Heisenberg, C. P. Multiscale force sensing in development. *Nat Cell Biol* **19**, 581-588, doi:10.1038/ncb3524 (2017).

2 Malinova, T. S. & Huveneers, S. Sensing of Cytoskeletal Forces by Asymmetric Adherens Junctions. *Trends Cell Biol*, doi:10.1016/j.tcb.2017.11.002 (2017).

3 Roca-Cusachs, P., Conte, V. & Trepat, X. Quantifying forces in cell biology. *Nat Cell Biol* **19**, 742-751, doi:10.1038/ncb3564 (2017).

4 Ribeiro, A. J. *et al.* Contractility of single cardiomyocytes differentiated from pluripotent stem cells depends on physiological shape and substrate stiffness. *Proc Natl Acad Sci U S A* **112**, 12705-12710, doi:10.1073/pnas.1508073112 (2015).

5 Huang, D. L., Bax, N. A., Buckley, C. D., Weis, W. I. & Dunn, A. R. Vinculin forms a directionally asymmetric catch bond with F-actin. *Science* **357**, 703-706, doi:10.1126/science.aan2556 (2017).

6 Buckley, C. D. *et al.* Cell adhesion. The minimal cadherin-catenin complex binds to actin filaments under force. *Science* **346**, 1254211, doi:10.1126/science.1254211 (2014).

7 Altman, D., Sweeney, H. L. & Spudich, J. A. The mechanism of myosin VI translocation and its load-induced anchoring. *Cell* **116**, 737-749 (2004).

8 Purcell, T. J., Sweeney, H. L. & Spudich, J. A. A force-dependent state controls the coordination of processive myosin V. *Proc Natl Acad Sci U S A* **102**, 13873-13878, doi:10.1073/pnas.0506441102 (2005).

9 Fenn, W. O. A quantitative comparison between the energy liberated and the work performed by the isolated sartorius muscle of the frog. *J Physiol* **58**, 175-203 (1923).

10 Greenberg, M. J., Shuman, H. & Ostap, E. M. Inherent force-dependent properties of beta-cardiac myosin contribute to the force-velocity relationship of cardiac muscle. *Biophys J* **107**, L41-44, doi:10.1016/j.bpj.2014.11.005 (2014).

11 Sung, J. *et al.* Harmonic force spectroscopy measures load-dependent kinetics of individual human beta-cardiac myosin molecules. *Nat Commun* **6**, 7931, doi:10.1038/ncomms8931 (2015).

12 Capitanio, M. *et al.* Ultrafast force-clamp spectroscopy of single molecules reveals load dependence of myosin working stroke. *Nat Methods* **9**, 1013-1019, doi:10.1038/nmeth.2152 (2012).

13 Veigel, C., Molloy, J. E., Schmitz, S. & Kendrick-Jones, J. Load-dependent kinetics of force production by smooth muscle myosin measured with optical tweezers. *Nat Cell Biol* **5**, 980-986, doi:10.1038/ncb1060 (2003).

14 Veigel, C., Schmitz, S., Wang, F. & Sellers, J. R. Load-dependent kinetics of myosin-V can explain its high processivity. *Nat Cell Biol* **7**, 861-869, doi:10.1038/ncb1287 (2005).

15 Laakso, J. M., Lewis, J. H., Shuman, H. & Ostap, E. M. Myosin I can act as a molecular force sensor. *Science* **321**, 133-136, doi:10.1126/science.1159419 (2008).

16 Greenberg, M. J., Lin, T., Goldman, Y. E., Shuman, H. & Ostap, E. M. Myosin IC generates power over a range of loads via a new tension-sensing mechanism. *Proc Natl Acad Sci U S A* **109**, E2433-2440, doi:10.1073/pnas.1207811109 (2012).

17 Aksel, T., Choe Yu, E., Sutton, S., Ruppel, K. M. & Spudich, J. A. Ensemble force changes that result from human cardiac myosin mutations and a small-molecule effector. *Cell Rep* **11**, 910-920, doi:10.1016/j.celrep.2015.04.006 (2015).

18 Reiser, P. J., Portman, M. A., Ning, X. H. & Schomisch Moravec, C. Human cardiac myosin heavy chain isoforms in fetal and failing adult atria and ventricles. *Am J Physiol Heart Circ Physiol* **280**, H1814-1820 (2001).

19 Krenz, M. & Robbins, J. Impact of beta-myosin heavy chain expression on cardiac function during stress. *J Am Coll Cardiol* **44**, 2390-2397, doi:10.1016/j.jacc.2004.09.044 (2004).

20 Malik, F. I. *et al.* Cardiac myosin activation: a potential therapeutic approach for systolic heart failure. *Science* **331**, 1439-1443, doi:10.1126/science.1200113 (2011).

21 Kadota, S. *et al.* Ribonucleotide reductase-mediated increase in dATP improves cardiac performance via myosin activation in a large animal model of heart failure. *Eur J Heart Fail* **17**, 772-781, doi:10.1002/ejhf.270 (2015).

22 Regnier, M., Rivera, A. J., Chen, Y. & Chase, P. B. 2-deoxy-ATP enhances contractility of rat cardiac muscle. *Circ Res* **86**, 1211-1217 (2000).

23 Takagi, Y., Homsher, E. E., Goldman, Y. E. & Shuman, H. Force generation in single conventional actomyosin complexes under high dynamic load. *Biophys J* **90**, 1295-1307, doi:10.1529/biophysj.105.068429 (2006).

24 Teerlink, J. R. *et al.* Chronic Oral Study of Myosin Activation to Increase Contractility in Heart Failure (COSMIC-HF): a phase 2, pharmacokinetic, randomised, placebo-controlled trial. *Lancet* **388**, 2895-2903, doi:10.1016/S0140-6736(16)32049-9 (2016).

25 Liu, Y., White, H. D., Belknap, B., Winkelmann, D. A. & Forgacs, E. Omecamtiv Mecarbil modulates the kinetic and motile properties of porcine beta-cardiac myosin. *Biochemistry* **54**, 1963-1975, doi:10.1021/bi5015166 (2015).

26 Swenson, A. M. *et al.* Omecamtiv Mecarbil Enhances the Duty Ratio of Human beta-Cardiac Myosin Resulting in Increased Calcium Sensitivity and Slowed Force Development in Cardiac Muscle. *J Biol Chem* **292**, 3768-3778, doi:10.1074/jbc.M116.748780 (2017).

27 Rohde, J. A., Thomas, D. D. & Muretta, J. M. Heart failure drug changes the mechanoenzymology of the cardiac myosin powerstroke. *Proc Natl Acad Sci U S A* **114**, E1796-E1804, doi:10.1073/pnas.1611698114 (2017).

28 Kron, S. J., Uyeda, T. Q., Warrick, H. M. & Spudich, J. A. An approach to reconstituting motility of single myosin molecules. *J Cell Sci Suppl* **14**, 129-133 (1991).

29 Adhikari, A. S. *et al.* Early-Onset Hypertrophic Cardiomyopathy Mutations Significantly Increase the Velocity, Force, and Actin-Activated ATPase Activity of Human beta-Cardiac Myosin. *Cell Rep* **17**, 2857-2864, doi:10.1016/j.celrep.2016.11.040 (2016).

30 Sommese, R. F. *et al.* Molecular consequences of the R453C hypertrophic cardiomyopathy mutation on human beta-cardiac myosin motor function. *Proc Natl Acad Sci U S A* **110**, 12607-12612, doi:10.1073/pnas.1309493110 (2013).

31 Nag, S. *et al.* Contractility parameters of human beta-cardiac myosin with the hypertrophic cardiomyopathy mutation R403Q show loss of motor function. *Sci Adv* **1**, e1500511, doi:10.1126/sciadv.1500511 (2015).

32 Walcott, S., Warshaw, D. M. & Debold, E. P. Mechanical coupling between myosin molecules causes differences between ensemble and single-molecule measurements. *Biophys J* **103**, 501-510, doi:10.1016/j.bpj.2012.06.031 (2012).

33 Planelles-Herrero, V. J., Hartman, J. J., Robert-Paganin, J., Malik, F. I. & Houdusse, A. Mechanistic and structural basis for activation of cardiac myosin force production by omecamtiv mecarbil. *Nat Commun* **8**, 190, doi:10.1038/s41467-017-00176-5 (2017).

34 Schmitt, J. P. *et al.* Cardiac myosin missense mutations cause dilated cardiomyopathy in mouse models and depress molecular motor function. *Proc Natl Acad Sci U S A* **103**, 14525-14530, doi:10.1073/pnas.0606383103 (2006).

35 Ho, C. Y. *et al.* Assessment of diastolic function with Doppler tissue imaging to predict genotype in preclinical hypertrophic cardiomyopathy. *Circulation* **105**, 2992-2997 (2002).

36 Tang, W. *et al.* Modulating Beta-Cardiac Myosin Function at the Molecular and Tissue Levels. *Front Physiol* **7**, 659, doi:10.3389/fphys.2016.00659 (2016).

37 Spudich, J. A. The myosin mesa and a possible unifying hypothesis for the molecular basis of human hypertrophic cardiomyopathy. *Biochem Soc Trans* **43**, 64-72, doi:10.1042/BST20140324 (2015).

38 Nag, S. *et al.* The myosin mesa and the basis of hypercontractility caused by hypertrophic cardiomyopathy mutations. *Nat Struct Mol Biol* **24**, 525-533, doi:10.1038/nsmb.3408 (2017).

39 Trivedi, D. V., Adhikari, A. S., Sarkar, S. S., Ruppel, K. M. & Spudich, J. A. Hypertrophic cardiomyopathy and the myosin mesa: viewing an old disease in a new light. *Biophys Rev*, doi:10.1007/s12551-017-0274-6 (2017).

40 Kampourakis, T., Zhang, X., Sun, Y. B. & Irving, M. Omecamtiv Mercabil and Blebbistatin modulate cardiac contractility by perturbing the regulatory state of the myosin filament. *J Physiol*, doi:10.1113/JP275050 (2017).

41 Kawana, M., Sarkar, S. S., Sutton, S., Ruppel, K. M. & Spudich, J. A. Biophysical properties of human beta-cardiac myosin with converter mutations that cause hypertrophic cardiomyopathy. *Sci Adv* **3**, e1601959, doi:10.1126/sciadv.1601959 (2017).

42 Trybus, K. M. Biochemical studies of myosin. *Methods* **22**, 327-335, doi:10.1006/meth.2000.1085 (2000).

Acknowledgments. The authors thank all members of the Spudich lab, D. Herschlag, R. McDowell, S. Nag, and J. Sung for discussions and/or edits to the manuscript. We thank MyoKardia, Inc. for providing the various small molecule effectors of the human β-cardiac myosin that were derived from their screens, dATP, and bovine actin. C.L. performed single molecule experiments and analyzed the data. M.K. performed in vitro motility experiments and analyzed the data. C.L. and D.S. performed ATPase experiments. D.S. analyzed the ATPase data. M.K., D.S., and K.M.R. expressed and purified protein. C.L. and J.A.S. wrote the paper. All authors discussed the data as it evolved and reviewed and edited the paper. This work was funded by NIH grants RO1GM033289 (J.A.S.), RO1HL117138 (J.A.S.), T32GM007276 (C.L.), TL1RR025742 (C.L.), and F32HL124883 (M.K.); Stanford Bio-X fellowship (C.L.); and Stanford School of Medicine Dean's Postdoctoral Fellowship (D.S.). The content is solely the responsibility of the authors and does not necessarily represent the official view of the National Institutes of Health.

Competing interests. J.A.S. is a founder of Cytokinetics and MyoKardia and a member of their advisory boards. K.M.R. is a member of the MyoKardia scientific advisory board.

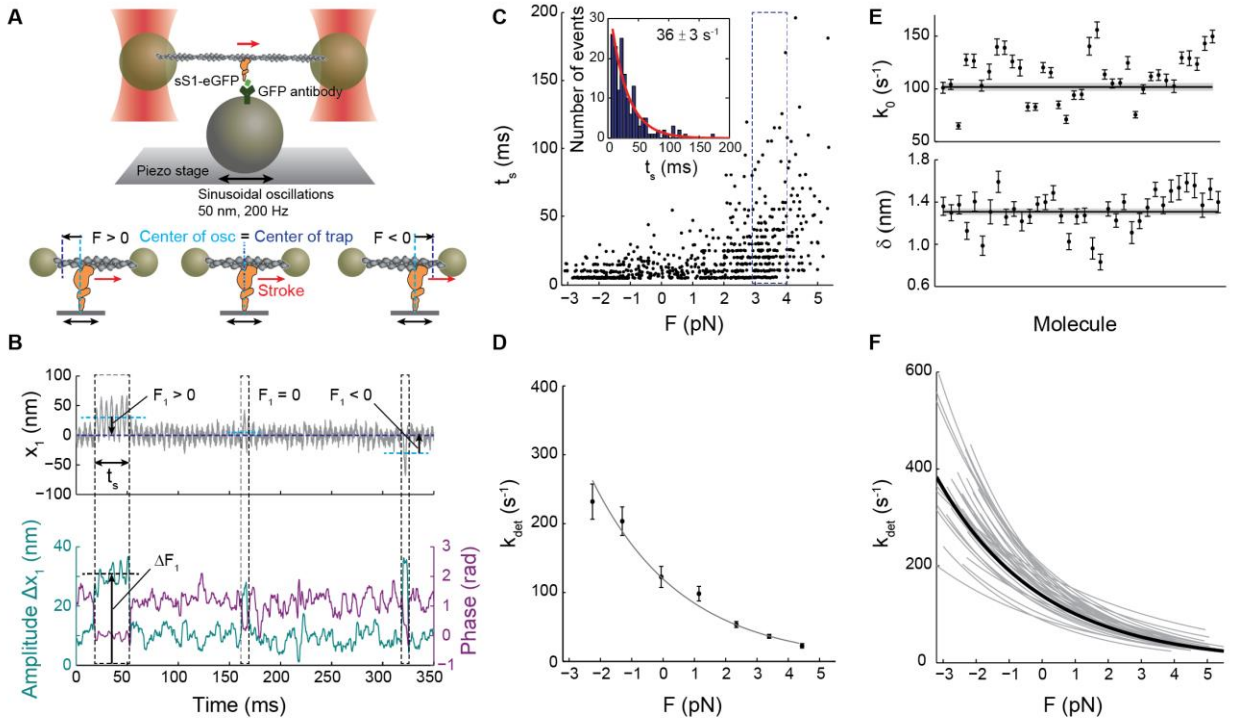

Fig. 1. Load-dependent kinetics of single molecules of human β-cardiac myosin measured by harmonic force spectroscopy. (A) Oscillations of the piezo stage on which myosin is attached in the three-bead optical trap system (top) apply an immediate sinusoidal load (force) to myosin upon attachment to actin (bottom). **(B)** Example trace of the position of one trapped bead, x_1 (top). An increase in the amplitude of oscillation and a simultaneous decrease in the phase between the trapped bead and piezo stage (bottom) are the two criteria used in the automated detection of an event. Over the course of many individual binding events, a range of forces with mean F_1 (calculated as the position x_1 multiplied by the trap stiffness) is automatically applied as myosin attaches randomly along the actin dumbbell to experience both positive (resistive) or negative (assistive) loads [11]. Three events are outlined, the first with positive F_1, the second with F_1 close to zero, and the third with negative F_1. Each event experiences the oscillatory force with mean F_1 and amplitude ΔF_1, calculated as the amplitude Δx_1 multiplied by the trap stiffness. Force F in Eqn. 1 is calculated as the sum of F_1 and F_2 from the second trapped bead, and the force amplitude ΔF is calculated as the sum of ΔF_1 and ΔF_2. **(C)** All events (N=729) for one example molecule. Duration of event (t_s) is plotted against force. Events binned by force (blue outline) have exponentially-distributed binding times from which the detachment rate at that force is determined by maximum likelihood estimation (MLE) (inset). The error on the rate is calculated from the variance of the MLE as the inverse Fisher information. **(D)** The force-dependent Arrhenius equation with harmonic force correction (Eqn. 1) is fitted to the detachment rates at each force to yield the load-dependent kinetics curve for one molecule. The two fitting parameters are $k_0 = 84 \pm 4$ s^{-1}, the rate at zero load, and $\delta = 1.31 \pm 0.03$ nm, the distance to the transition state, which is a measure of force sensitivity. Errors on k_0 and δ are from the covariance matrix (inverse Fisher information matrix) for the parameters. **(E)** k_0 (top) and δ (bottom) for all molecules measured (N=36). Their weighted means, $k_0 = 102 \pm 4$ s^{-1}, $\delta = 1.31 \pm 0.03$ nm, are shown as horizontal lines with s.e.m. in gray. **(F)** Load-dependent

kinetics curves for all molecules measured (gray), each described by a (k_0, δ) pair in (E). Individual data points as in (D) are not shown for clarity. The curve corresponding to the weighted means of k_0 and δ is shown in black. All experiments were done at saturating (2 mM) ATP.

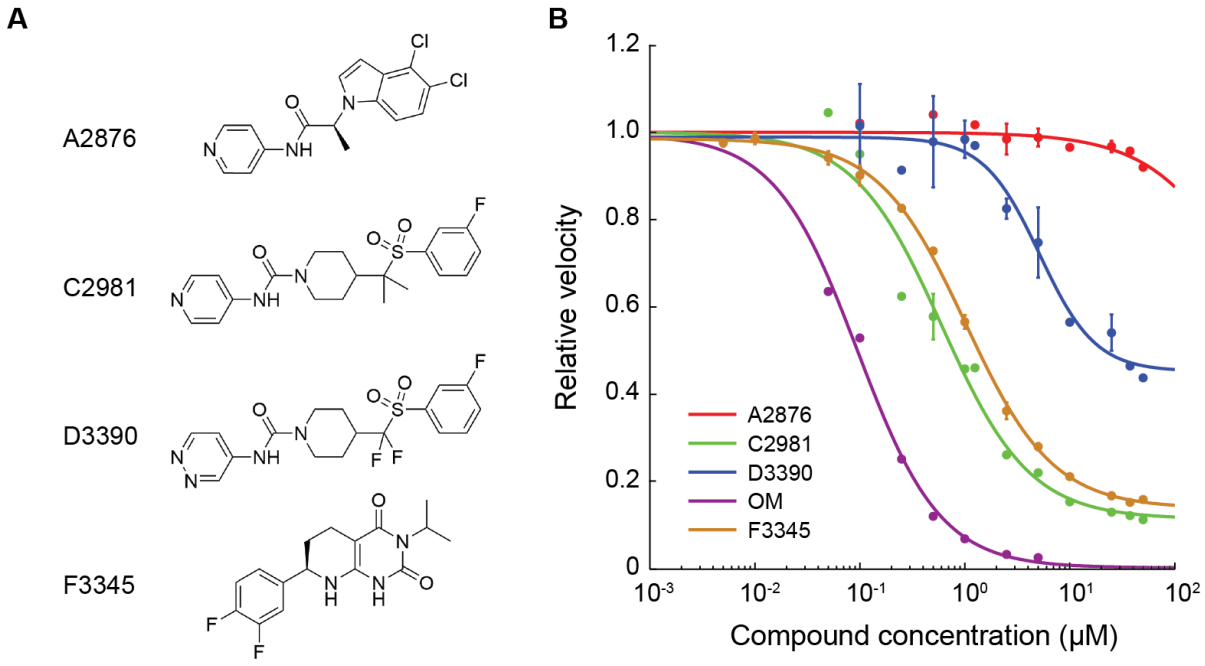

Fig. 2. Dose-dependent effects of small molecule compounds on the actin-sliding velocity of human β-cardiac myosin in unloaded in vitro motility. (A) Structures of the compounds used in this study. The structure of omecamtiv mecarbil (OM) is reported in Malik et al. [20]. **(B)** Dose-dependent effects of the compounds on the actin-sliding velocity of human β-cardiac myosin. Velocities are normalized to the value at zero compound concentration. Note that some data points have error bars smaller than the displayed point. Error bars represent s.e.m. between experiments, each tracking ~400 to ~1900 actin filament movements. Curves are 4-parameter logistic fits.

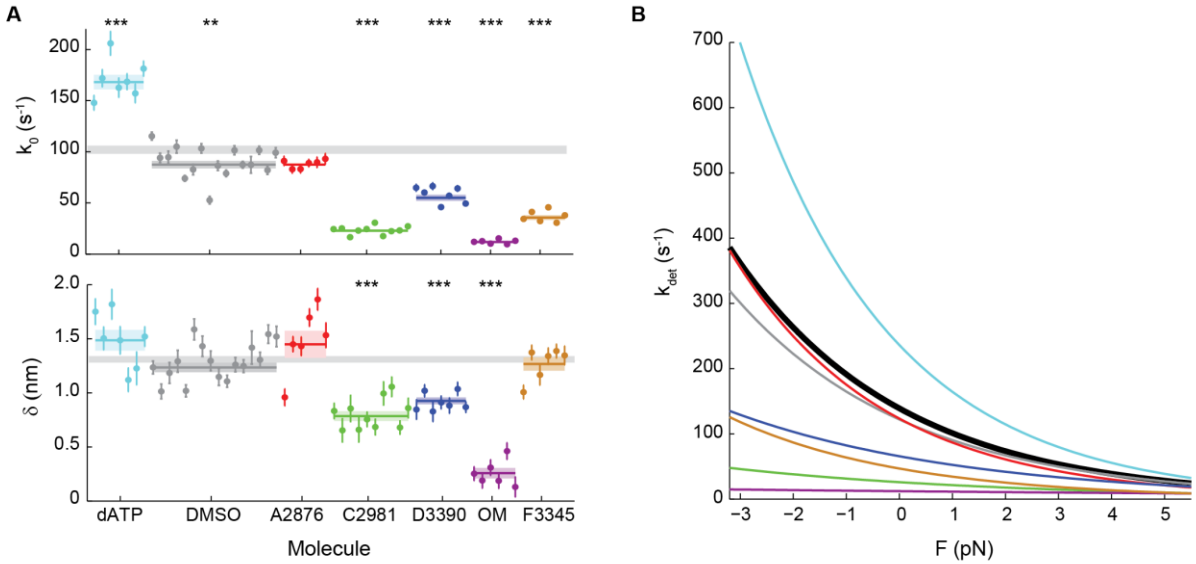

Fig. 3. Effects of small molecule compounds on the load-dependent kinetics of single molecules of β-cardiac myosin. (A) k_0 (top) and δ (bottom) for all molecules measured. Note that some molecules have error bars smaller than the displayed data point. Weighted means ± s.e.m. are shown as horizontal lines and shaded areas, with those of untreated myosin shown as gray bars (replicated from Fig. 1) across the plots. In the case of 2-deoxy-ATP (dATP), 2 mM dATP was used in place of ATP. All other conditions used 2 mM ATP, 2% DMSO, and 25 μM compound concentration. 2-tailed unequal variances t-test was performed on dATP vs ATP, DMSO vs WT, and compounds vs DMSO. **p<0.001, ***p<0.0001. For detailed values, see Tables 1 and S1. **(B)** The exponential dependence of detachment rate k_{det} on force for every compound. Curves correspond to the weighted means of k_0 and δ (see Fig. S2 for curves of individual molecules). Myosin without treatment is shown in black. The characteristic load-dependent kinetics curve of cardiac myosin is modulated to a gradient of degrees on the single molecule level by the compounds.

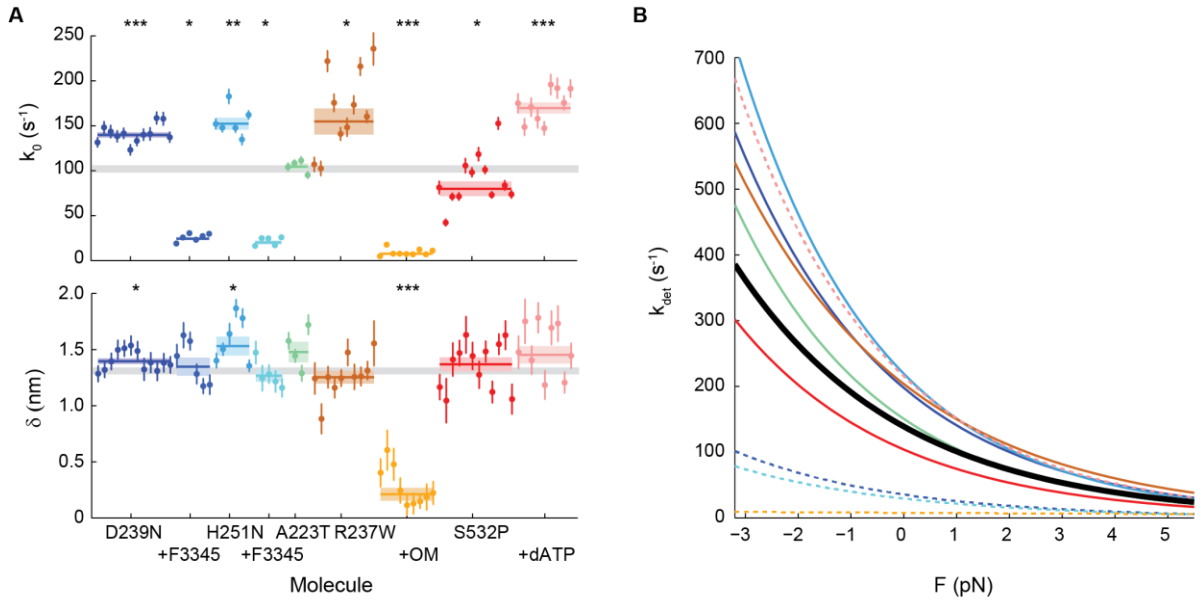

Fig. 4. Effects of cardiomyopathy-causing mutations on the load-dependent kinetics of single molecules of β-cardiac myosin, and their reversal by small molecule compounds. (A) k_0 (top) and δ (bottom) for all molecules measured. Note that some molecules have error bars smaller than the displayed data point. Weighted means ± s.e.m. are shown as horizontal lines and shaded areas, with those of untreated WT myosin shown as gray bars (replicated from Fig. 1) across the plots. Compound F3345, a cardiac myosin inhibitor, was used on the HCM mutants D239N and H251. No treatment was applied to the DCM mutant A223T which showed no significant change from WT. The cardiac myosin activator OM was used on the DCM mutant R237W. Addition of allosteric compounds were always in presence of 2% DMSO. Treatment for the DCM mutant S532P was using 2 mM dATP in place of ATP. 2-tailed unequal variances t-test was performed on mutants vs WT and mutants + compounds + DMSO vs mutants + DMSO, or S532P + ATP vs S532P + dATP. *p<0.05, **p<0.001, ***p<0.0001. For detailed values, see Tables 1 and S1. **(B)** The exponential dependence of detachment rate k_{det} on force for every mutant. Curves correspond to the weighted means of k_0 and δ (see Fig. S3 for curves of individual molecules). WT is shown in black. Dashed lines are mutants with treatment. Mutations modulate the load-dependent kinetics curve of cardiac myosin on the single molecule level to varying degrees, and their effects can be reversed by treatment with compounds.

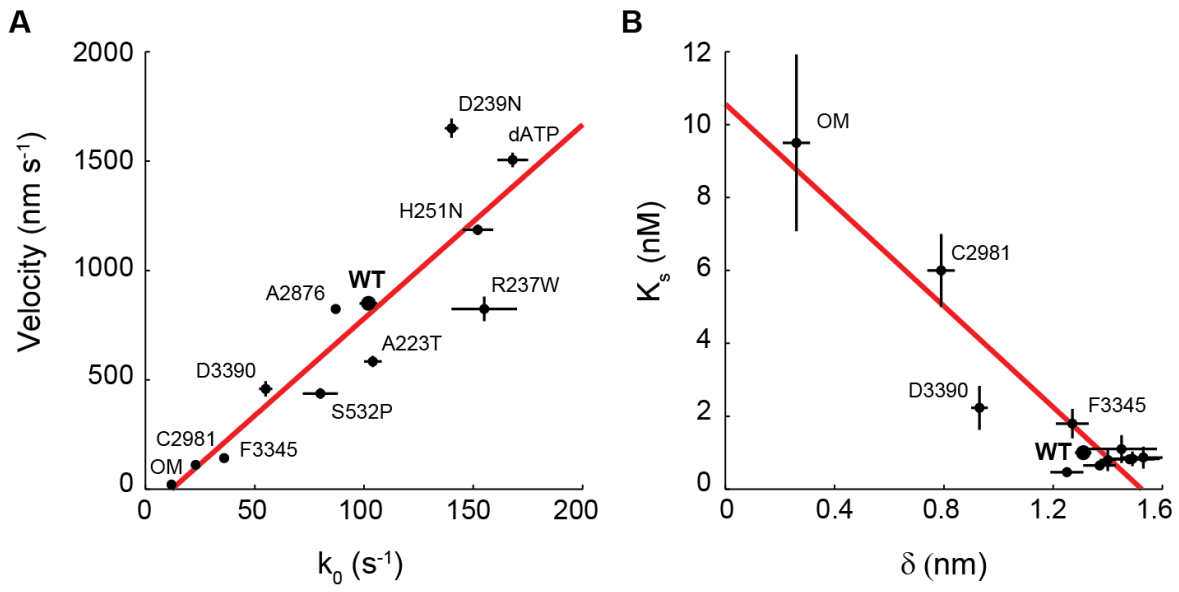

Fig. 5. Single molecule load-dependent kinetics as the basis of the ensemble force-velocity relationship in β-cardiac myosin. (A) Unloaded actin sliding velocity measured by in vitro motility assay vs. k_0, the detachment rate at zero load for a single molecule of myosin, for the compounds and mutations studied. The rate of detachment limits ensemble velocity. Linear regression gives a slope of 8.9 nm and $R^2 = 0.81$. Note that some points have error bars smaller than the dot. **(B)** The parameter K_s from the loaded motility assay is a measure of load-bearing ability at the ensemble level, while δ is the load-sensitivity parameter determined at the single molecule level. Pearson correlation -0.94. For clarity, the cluster of data points at the lower right corner are not individually labeled. Motility velocity and K_s values of HCM, DCM, and dATP are obtained from other studies [17,22,29] (Choe E., Spudich J.A., and Ruppel K.M., unpublished results; Tomasic I., Liu C., Rodriguez H., Spudich J.A., Bartholomew Ingle S.R., manuscript in preparation).

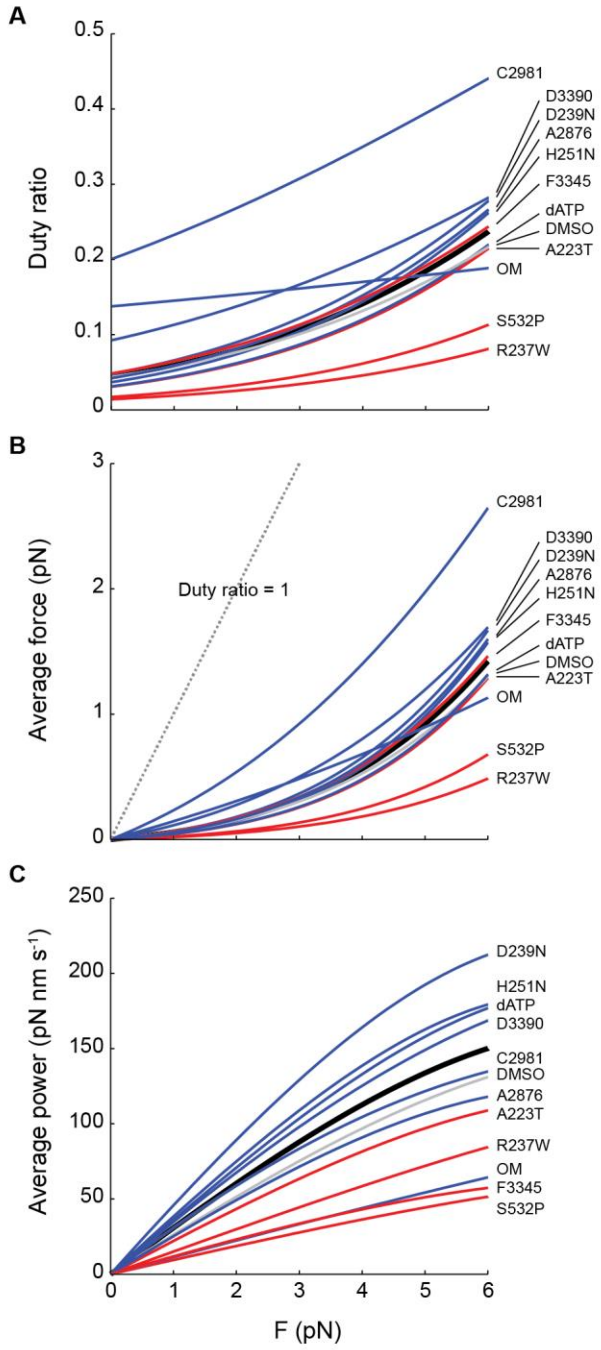

Fig. 6. The effects of small molecule compounds and cardiomyopathy-causing mutations on the load-dependent power production of single molecules of β-cardiac myosin. (A) Duty ratio, **(B)** average force, and **(C)** average power as a function of the load force F, calculated by Eqns. 2-5. All curves are calculated using values of detachment rate kinetics (k_0, δ), k_{cat}, and k_{attach} given in Table 1. Black: WT. Gray: DMSO. Blue: HCM and activators. Red: DCM and inhibitor.

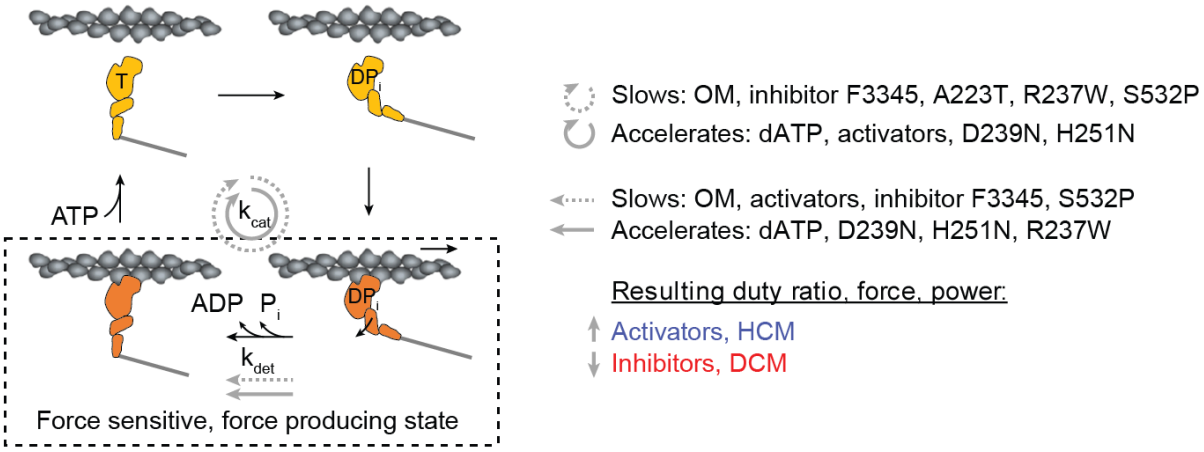

Fig. 7. Model of the effects of small molecule compounds and cardiomyopathy-causing mutations on the contractility of β-cardiac myosin at the single molecule level. The overall cycle, described by k_{cat}, can be slowed or accelerated by activators, inhibitors, HCM, and DCM mutations. Likewise, time spent in the strongly bound, force sensitive, force producing state can also be prolonged or shortened by these perturbations. It is the aggregate effects on the parameters of power production which discriminates activating (small molecule activators, HCM mutations) from inhibitory perturbations (small molecule inhibitors, DCM mutations).

	k_0 (s^{-1})	δ (nm)	k_{cat} (s^{-1})	k_{attach} (s^{-1})
WT	102 ± 4	1.31 ± 0.03	4.5 ± 0.4	4.7 ± 0.5
+dATP	168 ± 7 ***	1.49 ± 0.10	5.2 ± 0.4 *	5.4 ± 0.4
+DMSO	87 ± 4 **	1.24 ± 0.04	3.8 ± 0.1	4.0 ± 0.1
+A2876	87 ± 2	1.45 ± 0.13	3.7 ± 0.1	3.8 ± 0.1
+C2981	23 ± 1 ***	0.79 ± 0.05 ***	4.6 ± 0.1 *	5.7 ± 0.2
+D3390	55 ± 3 ***	0.93 ± 0.03 ***	5.1 ± 0.1 *	5.6 ± 0.1
+OM	12 ± 1 ***	0.26 ± 0.05 ***	1.6 ± 0.1 *	1.9 ± 0.1
+F3345	36 ± 2 ***	1.27 ± 0.06	1.7 ± 0.1 *	1.8 ± 0.1
D239N	140 ± 3 ***	1.40 ± 0.03 *	6.7 ± 0.5 *	7.0 ± 0.5
H251N	152 ± 7 **	1.53 ± 0.08 *	5.6 ± 0.4 *	5.8 ± 0.4
A223T	104 ± 4	1.48 ± 0.09	3.2 ± 0.2 *	3.3 ± 0.3
R237W	155 ± 15 *	1.25 ± 0.06	2.2 ± 0.4 *	2.2 ± 0.4
S532P	80 ± 8 *	1.37 ± 0.06	1.4 ± 0.1 *	1.4 ± 0.1

Table 1. Summary of single molecule detachment kinetics (k_0, δ) and actin-activated ATPase (k_{cat}) data for human β-cardiac myosin with effects of small molecule compounds and cardiomyopathy-causing mutations. Values are mean ± s.e.m. The attachment rate k_{attach} is calculated by Eqn. 3, with propagated error. Values given in this table are used in Fig. 6. k_{cat} of mutants are obtained from other studies [17,29] (Choe E., Spudich J.A. and Ruppel K.M., unpublished results). In the case of dATP, 2 mM dATP was used in place of ATP. All other conditions used 2 mM ATP, 2% DMSO, and 25 μM compound concentration. 2-tailed unequal variances (for k_0 and δ) and paired (for k_{cat}) (see Methods) t-test performed on dATP vs ATP, DMSO vs WT, compounds + DMSO vs DMSO alone, and mutants vs WT. *$p < 0.05$, **$p < 0.001$, ***$p < 0.0001$. For values and number of molecules of all conditions measured, see Table S1. Mean and s.e.m. of k_{cat}'s are from two protein preparations with 5-7 replicates for each condition (see Fig. S5 and methods).

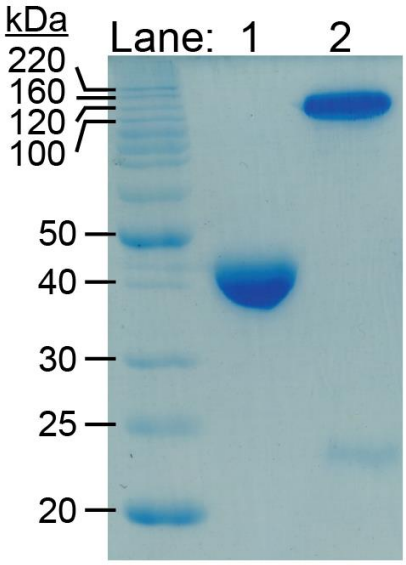

Fig. S1. Purified actin and myosin shown by SDS-PAGE. Lane 1 contains bovine cardiac actin (MW = 42 kDa) used in the actin-activated ATPase assay. Lane 2 contains recombinant human β-cardiac myosin sS1 (residue 1-808) fused to a C-terminal eGFP that migrates around 120 kDa. Myosin sS1 fragment was co-purified with a FLAG-tagged human ventricular essential light chain in which the FLAG tag had been cleaved off by TEV protease and migrates around 22 kDa.

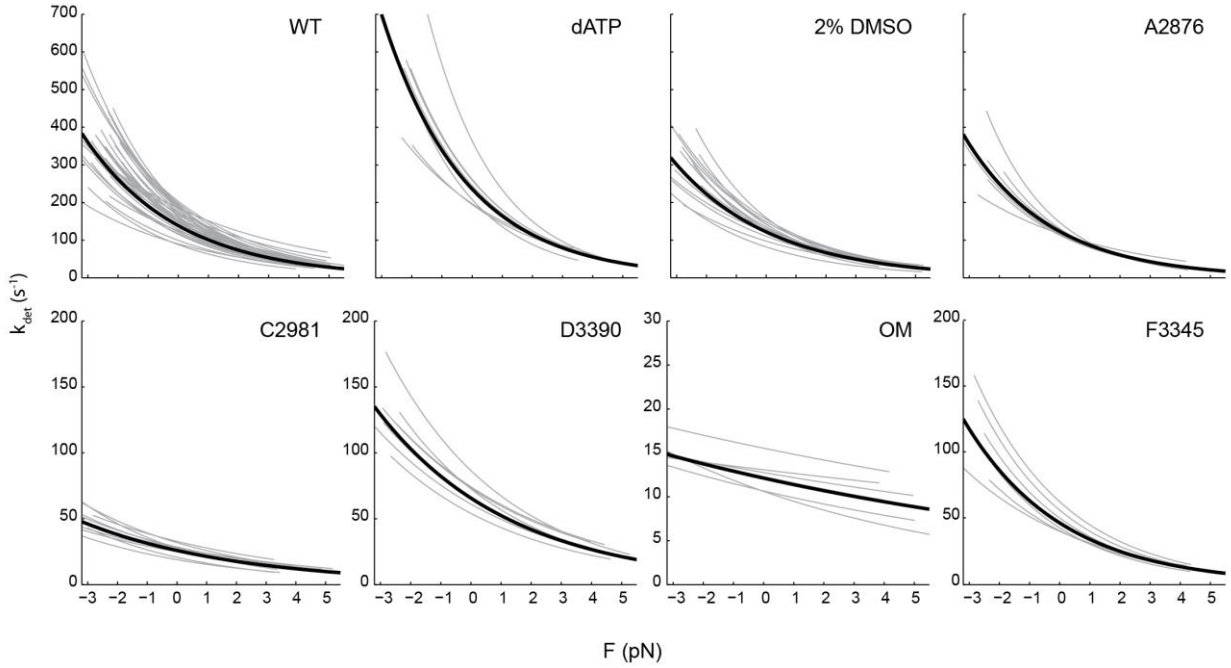

Fig. S2. Effects of small molecule compounds on the load-dependent kinetics of single molecules of human β-cardiac myosin. Each gray line represents one molecule. The weighted means of k_0 and δ across molecules for each condition have a curve represented in black and also plotted in Fig. 3B. Their values are given in Tables 1 and S1. The plot for WT is replicated from Fig. 1F for comparison. In the case of dATP, 2 mM dATP was used in place of ATP. All other conditions used 2 mM ATP, 2% DMSO, and 25 μM compound concentration.

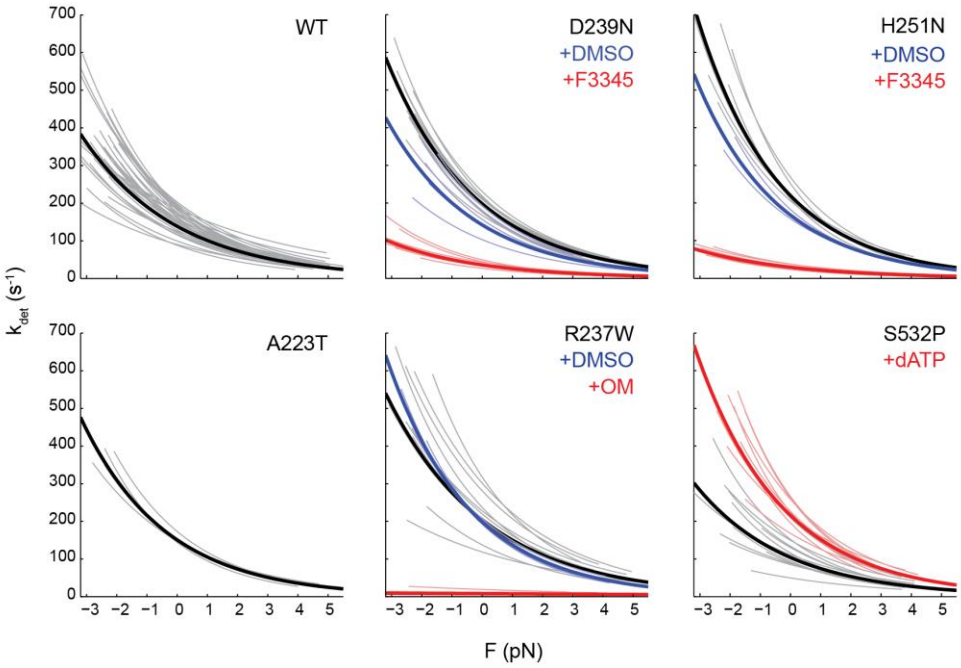

Fig. S3. Effects of cardiomyopathy-causing mutations on the load-dependent kinetics of single molecules of human β-cardiac myosin, and their reversal by small molecule compounds. Each thin line represents one molecule. The weighted means of k_0 and δ across molecules for each condition have a curve represented as a thick line and also plotted in Figure 4B. Their values are given in Tables 1 and S1. Addition of 25 μM compound F3345 to D239N and H251N and OM to R237W were in the presence of 2% DMSO, therefore effects of 2% DMSO (blue) on these mutants were also measured. Mutant A223T had no significant change from WT, therefore no compounds were added. The plot for WT is replicated from Fig. 1F for comparison.

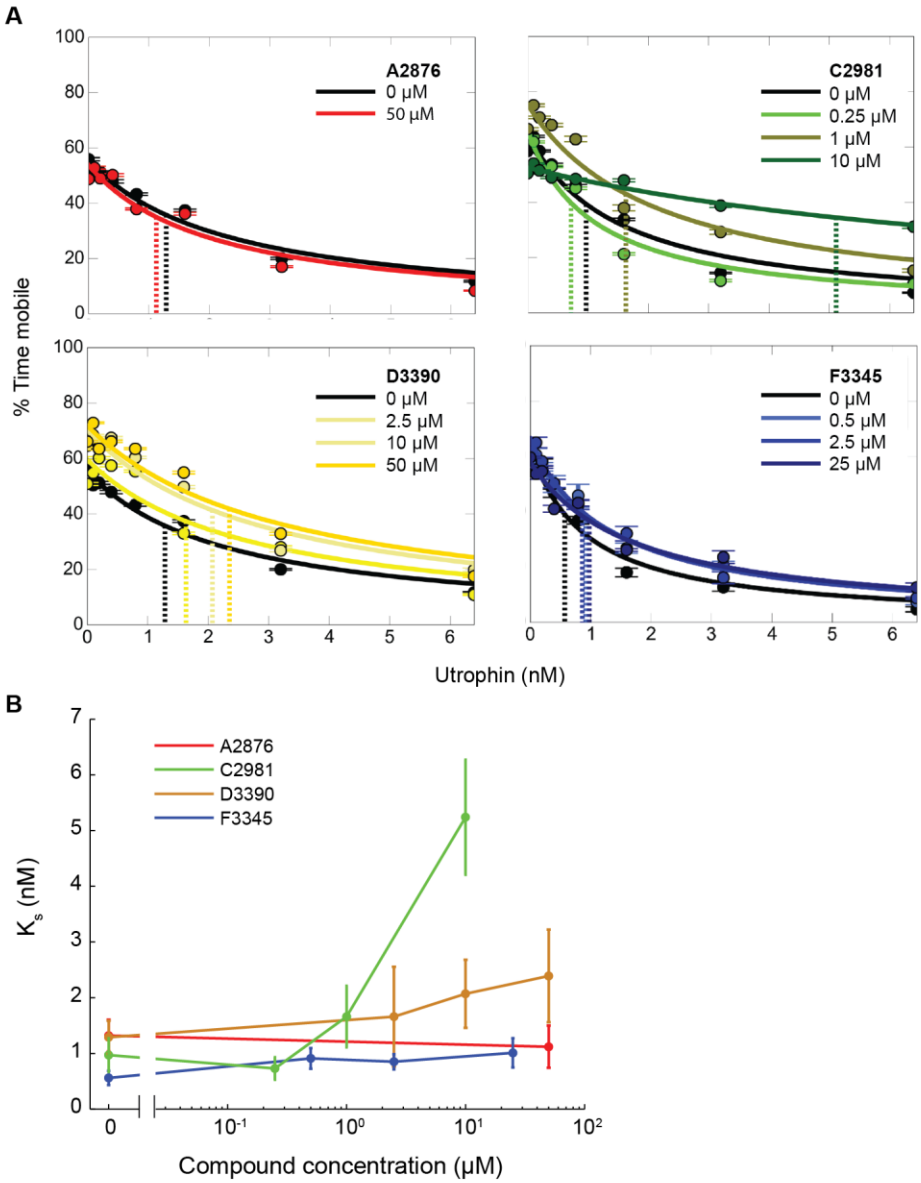

Fig. S4. Effects of compounds on the actin-sliding velocities of human β-cardiac myosin in the loaded in vitro motility. (A) Percent time mobile (a measure of velocity) as a function of the actin-binding protein utrophin, which served as a resistive load against myosin in the motility assay, as different concentrations of compound are added to WT myosin. Error bars represent s.e.m. of bootstrapped data calculated by the FAST program [17]. Dashed lines denote K_s, a measure of the ensemble load-bearing ability of myosin. K_s roughly corresponds to the concentration of utrophin required to slow down velocity by half (see [17] for rigorous definition). **(B)** K_s from (A) is plotted against compound concentration. Error bars represent s.e.m.

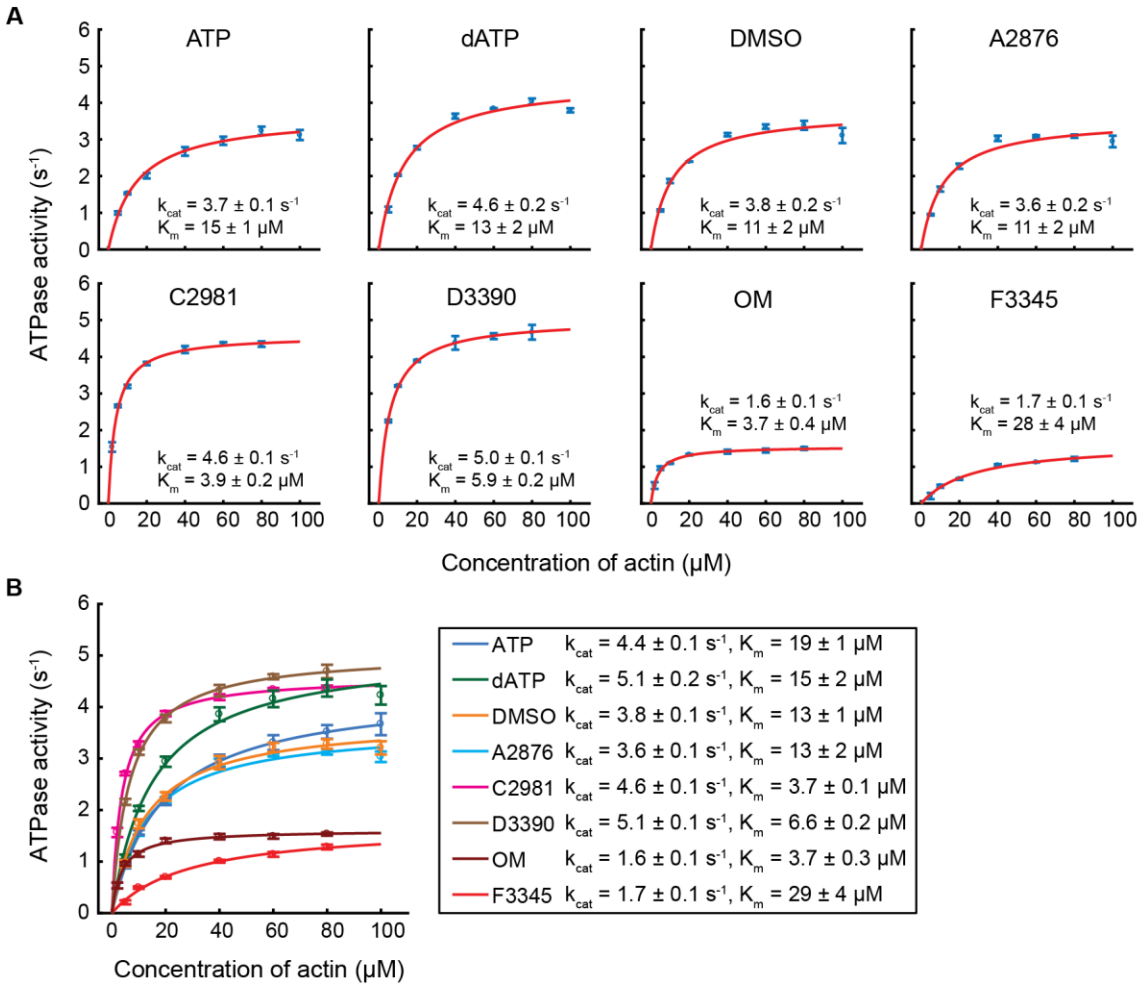

Fig. S5. Effects of compounds on the actin-activated ATPase of human β-cardiac myosin. **(A)** The Michaelis-Menten equation fitted to ATPase data for all conditions performed with one protein preparation. The entire experiment measuring all conditions was done on the same day that the protein was purified. Error bars on data points are s.e.m. of replicate experiments (n=3 in this example). Errors on k_{cat} and K_m are estimated fitting errors. k_{cat}'s from each day's experiment are averaged to calculate the mean and s.e.m. given in Table 1. **(B)** The Michaelis-Menten equation fitted to ATPase data aggregated from both protein preparations. Error bars on data points are s.e.m. of all replicates (total 5 - 7). Errors on k_{cat} and K_m are estimated fitting errors.

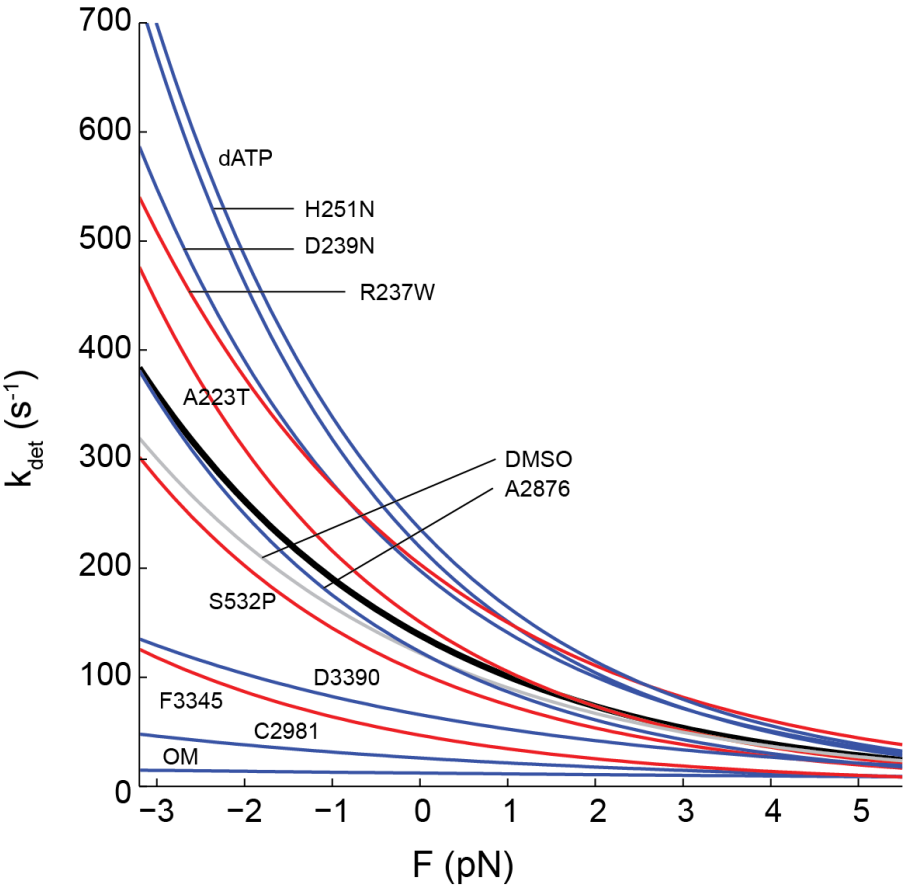

Fig. S6. Small molecule compounds and cardiomyopathy-causing mutations modulate the load-dependent kinetics of single cardiac myosin molecules across a spectrum. The weighted average detachment rate curves for the different conditions are replicated from Fig. 3 and 4. Their k_0 and δ values are given in Table 1. Black: WT. Gray: DMSO. Blue: HCM and activators. Red: DCM and inhibitor.

	k_0 (s^{-1})	p value	δ (nm)	p value	Number of molecules
WT	102 ± 4		1.31 ± 0.03		36
+dATP	168 ± 7	3.5e-5	1.49 ± 0.10	0.13	7
+DMSO	87 ± 4	1.4e-4	1.24 ± 0.04	0.59	16
+A2876	87 ± 2	0.60	1.45 ± 0.13	0.18	6
+C2981	23 ± 1	1.1e-12	0.79 ± 0.05	1.0e-7	10
+D3390	55 ± 3	1.7e-6	0.93 ± 0.03	7.7e-7	7
+OM	12 ± 1	4.0e-13	0.26 ± 0.05	4.0e-10	6
+F3345	36 ± 2	1.2e-10	1.27 ± 0.06	0.8	6
D239N	140 ± 3	3.1e-7	1.40 ± 0.03	0.04	12
+DMSO	108 ± 14	0.19	1.41 ± 0.04	0.74	5
+F3345	24 ± 2	0.0026	1.35 ± 0.08	0.71	6
H251N	152 ± 7	4.8e-4	1.53 ± 0.08	0.02	6
+DMSO	119 ± 4	0.0039	1.51 ± 0.09	0.60	2
+F3345	20 ± 2	0.0050	1.27 ± 0.05	0.17	5
A223T	104 ± 4	0.17	1.48 ± 0.09	0.13	4
R237W	155 ± 15	0.0039	1.25 ± 0.06	0.43	10
+DMSO	142 ± 4	0.12	1.51 ± 0.07	0.018	4
+OM	8 ± 1	2.4e-5	0.21 ± 0.06	1.0e-6	9
S532P	80 ± 8	0.021	1.37 ± 0.06	0.57	12
+dATP	170 ± 6	1.4e-7	1.45 ± 0.08	0.12	9

Table S1. Summary of single molecule detachment kinetics data (k_0, δ) for human β-cardiac myosin with effects of small molecule compounds and cardiomyopathy-causing mutations. Values are mean ± s.e.m. In the case of dATP, 2 mM dATP was used in place of ATP. All other conditions used 2 mM ATP, 2% DMSO, and 25 μM compound concentration. 2-tailed unequal variances t-test performed on dATP vs WT (ATP), DMSO vs WT, compounds + DMSO vs DMSO alone, mutants vs WT, and mutants + compounds + DMSO vs mutants + DMSO alone.